A Symmetric Ion-Lepton Collider for Jefferson Lab

S.A. Bogacz,[1] T. Horn,[1] F.J. Klein,[2] P. Nadel-Turoński[2]

[1] *Jefferson Lab, Newport News, VA and*

[2] *Catholic University of America, Washington, DC*

(Dated: November 5, 2008)

In order to fully explore the transition region from hadronic to partonic degrees of freedom, the capabilities of Jefferson Lab will eventually have to be extended beyond the 12 GeV upgrade. In particular, studies of hadron structure through exclusive reactions will require higher energies in order to reach higher Q^2 and lower x. This brief report proposes that the next Jefferson Lab upgrade focus on a medium-energy symmetric lepton-ion collider, optimized for exclusive reactions but offering a wide range of possibilities.

The collider would consist of two Figure-8 intersecting storage rings with about 1/2 - 2/3 the circumference of the CEBAF racetrack, for which the latter would be a lepton injector. On the ion side, a new SRF linac would be built, which could also serve as a prototype for Project X at Fermilab, and might be used for numerous applications. Since Jefferson Lab is already conducting extensive R&D for this project, this would naturally offer significant synergies. The injector would also have an accumulator ring doubling as a booster accelerating the ions up to the desired energy (matching the electron beam energy, limited by synchrotron radiation to 8-9 GeV) corresponding to about 170 GeV on a fixed target. The luminosity for 4 on 4 GeV/c $e-p$ collision would be well above 10^{33} cm^{-2} s^{-1} per interaction point (2×10^{34} using numbers from a very optimistic recent study of a COSY-based collider).

This proposal includes a staged construction plan, and presents opportunities for a variety of applications.

Contents

I. Executive Summary 3

II. Physics 5

A. Deep Processes 5

B. Hadron Spectroscopy 7

C. Inclusive and Semi-Inclusive Measurements 8

III. Detectors 9

A. General Considerations 9

B. Detector Example 11

1. Central Detector 11

2. Baryon Endcap 12

3. Electron Endcap 12

IV. Accelerator and Collider Complex 12

A. Injectors 13

B. Collider Rings 14

C. Interaction Regions 15

V. Staged Construction and Upgrade Plan 18

A. Option 1: Linac First 18

1. Proton Linac and Fixed Target Area 18

2. Collider with Unpolarized Ions 19

3. High-Luminosity Collider with Polarized Ions 19

4. Detector Upgrades 20

B. Option 2: Collider First 21

VI. Applications 22

A. Transmutation of Nuclear Waste 22

B. Long-Pulsed Spallation Neutron Source 22

C. Industrial Applications 23

VII. Adding COSY to CEBAF 23

References 26

I. EXECUTIVE SUMMARY

The 12 GeV upgrade will open up new possibilities for Jefferson Lab, in particular in the area of studying hadron structure through exclusive processes. However, to fully understand the transition region between hadronic and quark-gluon degrees of freedom one will eventually need to pursue measurements at higher Q^2 in the valence region, as well as at lower x, to map out the gluon and sea quark distributions. Moving beyond the charm threshold will also open up new opportunities for spectroscopy.

Going to higher energies, colliders become an attractive and cost effective alternative to fixed target experiments, offering low backgrounds (no Moller electrons), and a high figure of merit for (particularly transverse) polarization measurements. The symmetric case, when both beam particles have equal momentum, gives the lowest lab momenta for a given $\sqrt{s_{ep}}$, which translates into superior momentum resolution and particle identification (flavor tagging). Symmetric kinematics also improve the acceptance. The question is thus, should the next step for Jefferson Lab be an incremental increase in the capabilities of CEBAF, or should it be a major leap forward in the form of an electron ion collider? And if so, should the collider be geared towards semi-inclusive reactions at high energies or exclusive processes at medium energies, up to the limit imposed by the achievable detector resolution? The latter becomes a major challenge for exclusive processes approaching already $\sqrt{s} \sim 10$ GeV, and precision measurements would require a dedicated effort. Incidentally, this is also the region above which one cannot perform L/T separations, as ϵ goes to unity at high $\sqrt{s}$.

Since high-energy colliders, such as the proposed Electron Light-Ion Collider (ELIC) [2–4], cannot operate at medium energies (see discussion the design of the interaction region optics in Section IV C), Jefferson Lab will need to make a choice on what physics to pursue. In this document we present an option optimized for medium-energy exclusive processes. These include diffractive reactions, such as Deeply-Virtual Compton Scattering (DVCS) and ρ^0 or J/Ψ production, which allow imaging of quarks and gluons, and non-diffractive processes like production of pions, kaons, and charged ρ mesons, which give access to the spin/flavor structure of quark GPDs. High resolution would also be essential for expanding our understanding of QCD through exclusive polarization measurements in charmed baryon spectroscopy, but it would benefit all experiments. Section II provides a more extensive discussion of the physics opportunities.

The collider itself, described in Section IV, would consist of "Figure-8" [1] intersecting storage rings with four possible interaction points and a circumference of about 1/2 - 2/3 of the CEBAF racetrack. It would be based on the lattice architecture developed for ELIC, but it would be considerably simpler and would not depend on successful R&D of new technologies. While nominally designed for $e - p$ collisions of up to 8.8 on 9 GeV/c, corresponding to a fixed target electron energy of 170 GeV, it would be possible to inject ions with somewhat higher momenta. The electron energy is limited to CEBAF four pass beam (8.8 GeV) by synchrotron radiation.

The acceleration will be carried out by linacs, preserving low emittance for both beams. While CEBAF would be used for the electrons, a new 2 GeV SRF linac would be built for the ions. The latter would be based on the low-β section of the 8 GeV linac developed for Project X at Fermilab [7], in which Jefferson Lab SRF Institute is heavily involved. The common R&D effort would create significant synergies and allow cost-effective manufacture, with the Jefferson Lab linac becoming a prototype for Project X.

The secret to achieving a high luminosity in a collider lies in the injector. In order to reach Ampere range currents with polarized beams, bunch stacking and multiple stages of cooling are necessary. At low energy, electron cooling is the most effective. Thus, after the initial SRF linac with RFQ focusing, ions with an energy of about 300 MeV/u could be diverted into a small accumulator ring before heading for the booster ring. After electron cooling they would continue their accleration up to 2 GeV, taking advantage of the superb emittance preservation feature of a linac. On the other hand, ions intended for fixed targets could bypass the accumulator ring. In the booster ring, the ions would be accumulated up to a space charge limited emittance, and a first stage of stochastic cooling would be applied to the coasting beam, which would now have sufficiently high energy. The RF would then give the beam the correct time structure, and accelerate it to the desired energy. A second round of bunched beam stochastic cooling, currently being developed at RHIC, could then be applied to further reduce the emittance before injection into the collider ring.

With rather conservative assumptions for the normalized emittance, the proposed configuration would deliver a luminosity of at least 2×10^{33} cm^{-2} s^{-1} per interaction point already for 4 GeV/c protons. The latter is important as the luminosity in $e-p$ collisions increases with the proton energy. A more optimistic scenario, or progressive improvements in cooling technology or ion source currents, could significantly increase the luminosity beyond this nominal value. Using the very optimistic assumptions from a recent study of a COSY-based collider [11] would increase our luminosity to 2×10^{34} cm^{-2} s^{-1}.

A linac energy of 1 - 2 GeV is also ideal for a wide range of applications, some of which are discussed in Section VI. Reliable high-current, CW proton linacs constitute a key technology for accelerator-driven transmutation of nuclear waste, which may become a part of the solution in quest for energy independence and reduction of greenhouse gas emissions. The Jefferson Lab SRF proton linac would put the lab at the cutting edge of this technology. In parallel with serving as the injector of the collider, protons from the linac could also be used for fixed target experiments just as in the case of the CEBAF electron beam. Nuclear physics experiments with gas targets could run in parallel with, for instance, a long-pulse neutron spallation source, which would complement the short-pulsed one at the SNS [9]. Building such a facility in conjunction with the Jefferson Lab collider would offer performance in many ways comparable to the proposed European Spallation Source (ESS) [10], but at a small fraction of the cost.

II. PHYSICS

A. Deep Processes

Form factors and parton distributions probe the spatial and momentum structure of the nucleon in elastic and inelastic scattering respectively. These reactions have historically been discussed as separate concepts. Only recently was it realized that these in fact represent special cases of a more general way of describing the nucleon structure. The Wigner quantum phase space distributions are functions that simultaneously describe the position and momentum of particles in a quantum-mechanical system, and thus are the closest analogue to a classical phase space density that is allowed by the uncertainty principle. Experimentally, the Wigner functions are associated with Generalized Parton Distributions (GPDs), which contain all the information about the spatial (form factors) and momentum densities, as well as their correlations. Generalized Parton Distributions thus provide the most complete description of the structure of the nucleon, and allow quantifying the contribution of the orbital motion of quarks in the nucleon to the total nucleon spin.

Exclusive processes in $e-p$ scattering at collider energies can be either "diffractive" (no exchange of quantum numbers between the target and the projectile/produced system) or "non-diffractive" (where there is an exchange of quantum numbers). By measuring diffractive channels (J/Ψ, ρ^0, or ϕ production) at sufficiently high Q^2, one probes the gluon GPDs and/or the singlet quark GPD. In particular, J/Ψ production probes the gluon GPD in the nucleon, and its t-dependence reveals the transverse spatial distribution of the gluons. Measurements of DVCS and exclusive ρ^0 production at high Q^2 provide access to the singlet quark and gluon GPD.

Non-diffractive channels like π^+, π^0, or K^+ production are sensitive to the flavor and spin structure of the nucleon at small x, which complements the information obtained from DVCS and meson production experiments in the valence region. For moderate values of x, the proposed collider could reach $Q^2 > 10$ GeV^2, where higher-twist contributions, which complicate the extraction of GPDs from the data, are expected to be small. Indeed, the comparison of different meson channels alone provides model-independent information about the ratio of quark spin and spatial distributions, and a comparison between π^+ and K^+ production may allow studies of SU(3).

Figure 1 shows the accessible phase space for the $ep \to e'\pi^+ n$ reaction in 4 on 4 GeV/c and 8.8 on 9 Gev/c kinematics, while Figure 2, shows a prediction for the s- and t-dependence of the differential cross section at $x = 0.04$ for several values of Q^2. The higher energy pushes x down to 10^{-3} at low Q^2, but already around $\sqrt{s} \sim 8$ GeV, moderate values of Q^2 can be reached at relatively low x.

Access to the rich physics contained in GPDs requires that hard-soft factorization applies, and the cross section is dominated by longitudinal photons. For moderate values of Q^2, the only way to ensure this for non-diffractive channels is to extract the longitudinal and transverse

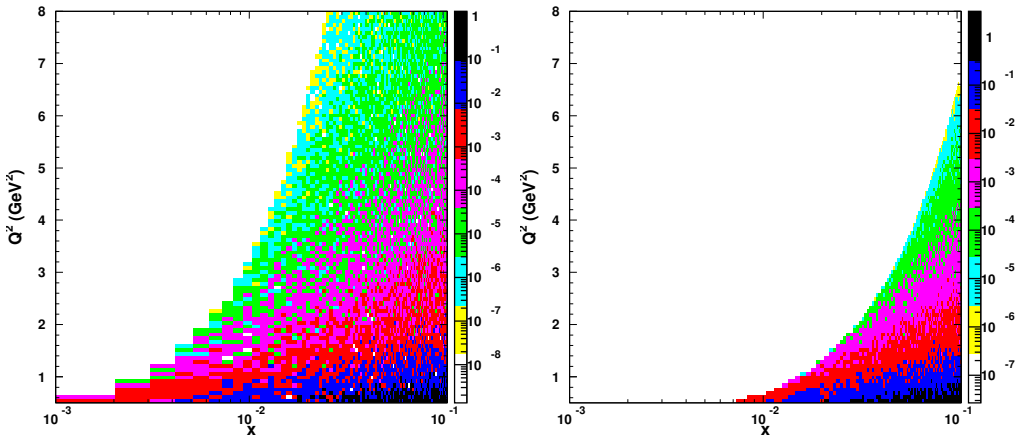

(a) *8.8 on 9 GeV/c* (b) *4 on 4 GeV/c*

FIG. 1: *Kinematic coverage for* $ep \to e'\pi^+ n$ *with* $x < 0.1$, $Q^2 > 0.5$ GeV^2, *and* $\theta_{e'} > 3^\circ$.

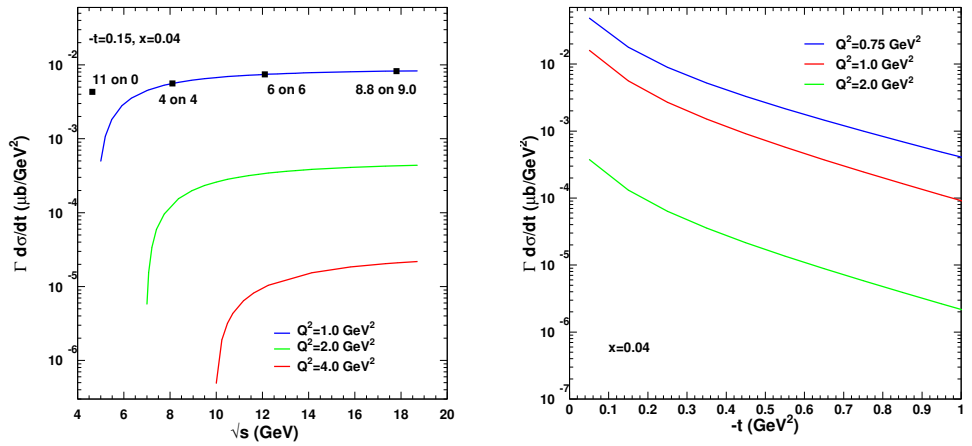

(a) . (b) *4 on 4 GeV/c*

FIG. 2: *s- and t-dependence of the* $ep \to e'\pi^+ n$ *cross section at* $x = 0.04$.

components of the cross section, which requires measurements at two sufficiently different values of the virtual photon polarization, ϵ. This powerful technique is, however, only applicable at medium energies ($\sqrt{s} \sim 10$ GeV) as ϵ goes to unity for all kinematics when the energy increases beyond the range of our proposed collider.

Compton scattering is considered the cleanest way to access GPDs, and a collider would also provide a unique opportunity to conduct the first double-DVCS experiments, *i.e.*, $\gamma^* N \to \gamma^* N \to$

e^+e^-N. This would allow probing valence quark GPDs for any kinematical point (x, ξ, t) where $x < |\xi|$, rather than being limited to the $x = \xi$ line as is the case for DVCS. This measurement is, however, particularly challenging not only because the cross sections are lower, but due to difficulties in distinguishing the scattered electron and the one coming from the decay of the timelike final-state photon. A collider would, however, allow detection of both electrons, and provide a kinematic separation of the two over the relevant ranges in Q^2 and $Q'^2 = m^2_{e^+e^-}$ (the latter preferably between 4 and 9 GeV^2).

Measurements of GPDs are challenging and require high luminosities, because one needs to measure exclusive reactions over a large kinematic range. The design of the detector and the interaction region thus have to provide sufficient resolution and acceptance for a proper reconstruction of the final state. Table I shows the missing mass resolution for different collision energies using a fixed momentum resolution of 1% for charged particles and 3% for neutral particle detection. Since the missing mass resolution depends not only on the detector resolution and momentum of the detected particles, but also on the available phase space, ensuring exclusivity becomes an experimental challenge as collision energies increase. This empasizes the need for dedicated experiments which can push the resolution limit in order to map out the nucleon structure through quark and gluon GPDs and understand the reaction mechanisms.

$e - p$ [GeV/c]	$e'\pi^+(n)$ [GeV] (a)	$e'\pi^+ n$ [GeV] (b)	$e'\gamma p$ [GeV] (c)
11 on 0	0.06	0.25	0.03
4 on 4	0.20	0.33	0.18
6 on 6	0.37	0.44	0.38
8.8 on 9	0.57	0.69	0.68

TABLE I: *Colum (a) shows the σ for the missing neutron mass reconstructed from $e'\pi^+$ in the $ep \to e'\pi^+ n$ reaction. Column (b) shows the corresponding uncertainty in the total missing mass squared (if all particles are detected) for the same reaction, and column (c) shows the corresponding uncertainty for DVCS. The simulation of the missing mass was done using a fixed momentum resolution of 1% for charged particles and 3% for neutral particles.*

B. Hadron Spectroscopy

Precise data on charmed baryons would be essential for bridging the gap between the domain of heavy quarks, where lattice QCD is close to producing a quantitative description of baryon structure, and the nucleon, where pioneering efforts are at best qualitative. The possibility to gain a detailed understanding the excited states of charmed hadrons from first principles, and exploring

exotic configurations similar to the $\Lambda(1405)$ "molecule", would not only advance the efforts towards a lattice QCD description of the nucleon, but in the short term also guide effective models used to interpret, for instance, the results of the Jefferson Lab N^* program.

The charm sector also offers the best opportunity to look for hybrid baryons with excited glue. While not as easily identified as their meson counterparts, many of which are expected to clearly exhibit exotic quantum numbers, the hybrid baryon states are nevertheless predicted by QCD, and their existence will eventually need to be confirmed. A combination of lattice QCD calculations and precision data on charmed baryons offers the most promising approach to resolving this question.

While there are efforts under way for, in particular, the spectroscopy of charmed mesons using hadronic probes or e^+e^- annihilation (for instance at CLEO [12]), the proposed collider would provide unique opportunities for polarization measurements in $e-N$ collisions. For quasi-real, low-Q^2 photons, it would in principle even possible to perform a complete measurement [13] of the $\gamma p \to D^0\Lambda_c^+$ channel, determining the four complex amplitudes of the process in a direct, model-independent way. Since the self-analyzing power of the $\Lambda_c^+ \to \Lambda\pi^+$ decay is -0.91 ± 0.15, ten polarization observables can be measured in addition to the cross section using circularly polarized photons from longitudinally polarized electrons, and both longitudinal and transvsersely polarized protons, in an effort similar to the one currently undertaken in Hall B for the $K\Lambda$ channel. While not all charmed baryons have self-analyzing decays, and statistics may be a limiting factor, polarization measurements using electromagnetic probes provide a powerful tool for testing our theoretical understanding of baryon structure and can reveal important clues for the development of lattice QCD.

C. Inclusive and Semi-Inclusive Measurements

Good resolution, acceptance, kinematic coverage, and flavor tagging also open up many opportunities for inclusive and semi-inclusive experiments. Some of the experiments are sensitive to the individual polarization of u, d, and s quarks and anti-quarks. They could provide important new information on the role of individual quarks in nucleon structure, for instance, determining whether or not all anti-quarks spin against the proton, counteracting the valence contribution and leading to the observed small total quark and anti-quark spin contribution.

Semi-inclusive measurements, in which certain hadrons in the final state are detected, allow for "tagging" the various quark or anti-quark flavors in the proton, and can provide precise measurements of the individual polarizations. Flavor tagging can be achieved easily in the symmetric kinematics of our proposed collider where the final state hadrons have relatively low energies. The technique becomes much more difficult at high ion momenta where hadrons have a high energy due to kinematics and not dynamics.

Measurements of inclusive spin-dependence structure functions in which W or Z bosons

are exchanged instead of a photon between the electron and the nucleon provide an alternative to those performed in conventional electromagnetic scattering. These exchanges violate parity and thus probe the spin-dependent quark and anti-quark distributions in different combinations. Such experiments could be performed with electrons and positrons, and would require the highest possible beam energies. Charge symmetry violation experiments would allow, through comparison of the e^+d with the e^-d current charged cross section, for tests of the charge symmetry sum rule of the sea, where effects are expected to be large [17].

III. DETECTORS

The four interaction points would make it possible to use several detector concepts tailored for specific the needs of various processes. However, before going into details, we will give a general overview.

A. General Considerations

Since the momentum resolution (dp/p) to first order scales linearly with the momentum, the best resolution is achieved by keeping the lab momenta as low as possible for a given $\sqrt{s_{ep}}$. This is achieved in a symmetric, or nearly symmetric collider. As illustrated in Figures 3 and 4 for the $ep \to e'\pi^+ n$ reaction, using a phenomenological parametrization by T. Horn, such kinematics also offer the advantage that the angular distribution of the outgoing electrons and mesons covers nearly 4π, providing the best angular resolution.

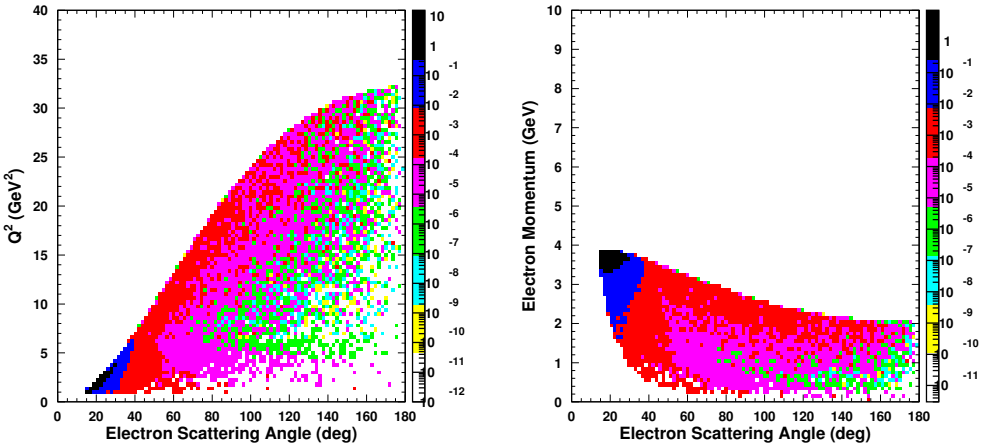

(a) Q^2 *vs. scattering angle* (b) p *vs. scattering angle*

FIG. 3: *4 on 4 GeV/c scattered electron kinematics.*

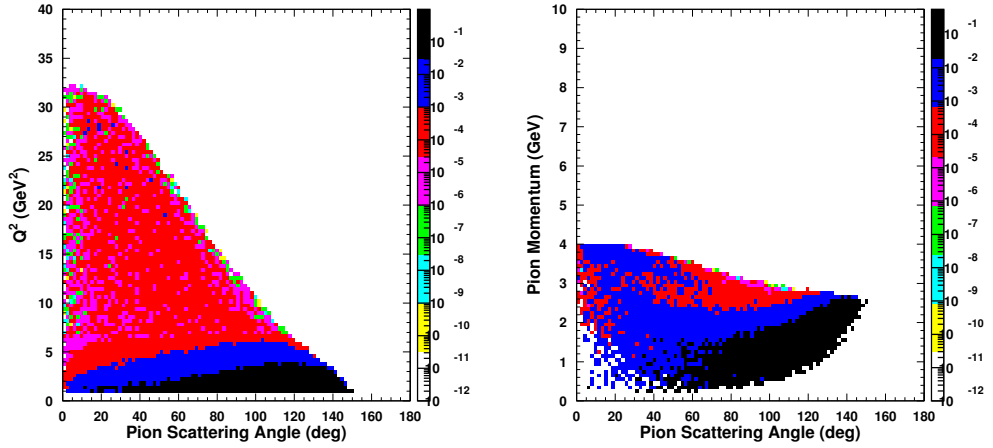

(a) Q^2 *vs. scattering angle* (b) p *vs. scattering angle*

FIG. 4: *4 on 4 GeV/c scattered pion kinematics.*

In $e-p$ collisions, the main challenge is that the outgoing baryons are scattered at relatively small angles, especially at low $-t$. This issue, shown in Figure 5, is difficult to address using only a solenoid, since the magnetic field is almost parallel to the direction of motion for the low-t particles, and hence the momentum resolution is poor. The obvious choice is to use a toroid that could bend positive particles outwards, allowing coverage down to angles of 2-3° or less with very high resolution. The downside of a torus, however, is that the coils reduce the acceptance at very forward angles, and produce holes in the ϕ coverage. A solenoid-torus combination will be discussed below, but a large torus similar to the CLAS detector and other configurations are also possible.

Besides kinematics, the other major factor guiding any detector setup is the design of the interaction region. Since our layout of the intersecting storage rings uses ELIC as a starting point, a comparison is pertinent. In ELIC, extreme focusing at the interaction point made it possible to increase the design luminosity by several orders of magnitude compared with conventional collider optics. This does, however, come at a price. The technical details will be covered in the accelerator section, but the detector related consequences were twofold. First, the space available for detectors is limited to 7.8 m end-to-end (quad-to-quad) [14]. In addition, the complex of quadrupoles, sextupoles, and special cavities for the crab crossing, make it difficult to use beamline dipoles in a spectrometer role. Thus, while the large boost in 9 on 225 GeV collisions make the baryons go down the beam pipe and mesons very close to it, there are only 3.9 m available on each side to accommodate detectors for tracking, identification, and calorimetry for particles with momenta of 10-100+ GeV/c, which have very considerable radii of curvature even in the strongest magnetic fields. Consequently, both the acceptance and resolution will suffer. Failure to reconstruct events

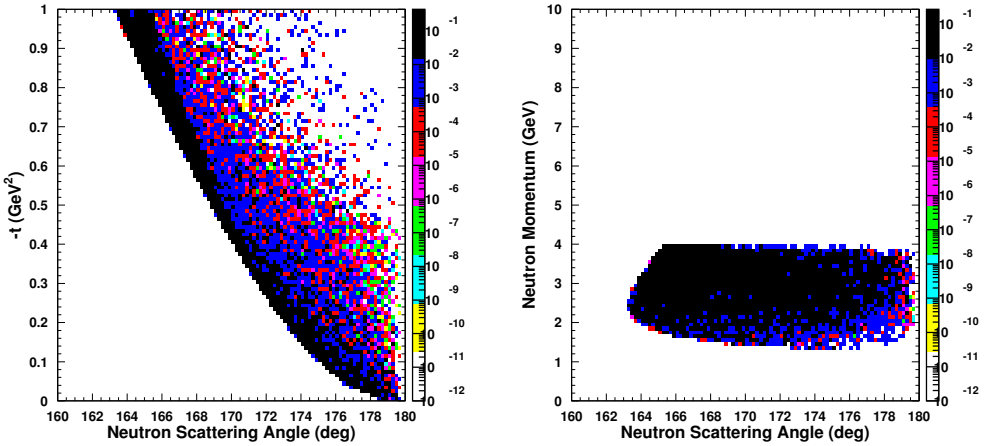

(a) $-t$ *vs. scattering angle*

(b) p *vs. scattering angle*

FIG. 5: *4 on 4 GeV/c scattered neutron kinematics.*

with high-momentum particles can dramatically reduce the data rate even if the luminosity is large. In contrast, the COMPASS detector, designed for a 200 GeV beam, is 60 m long (to one side) [15].

However, a symmetric collider makes it possible to employ asymmetric focusing, the details of which are described in Section IV, slightly extending the interaction region while retaining a very aggressive β^* for the ions. In our proposed collider, with momenta below 9 GeV/c, an interaction region of 8 m, comparable in size to the CLAS detector [16], would be sufficient.

B. Detector Example

As an example detector configuration, we will consider one based on a superconducting solenoid of about 5 m in length, 2 m in diameter, and with a field of 2-3 T, slightly shifted towards the (outgoing) electron side. On the (outgoing) baryon side, there will be an additional toroid bending out the trajectories of positive particles scattered at small angles.

1. Central Detector

The central detector would be placed inside and around the solenoid. At the center there would be a vertex detector. It would be surrounded by either drift chambers or time-projection chambers (TPC) for tracking. The latter can take advantage of experience from ALICE, where tests have shown a momentum resolution of 1% at 2 GeV/c in a solenoidal field of only 0.5 T [18]. While not required for exclusive reactions, particle identification for spectroscopy could be enhanced by

adding a Cerenkov detector outside of the tracking chambers. This particle identification system should be thin to minimize the impact on the resolution of subsequent detectors and to reduce the overall cost. Both criteria are met by a novel ring-imaging Cerenkov detector (Detector of Internally Reflected Cerenkov light, DIRC) developed and used successfully at BaBar [19]. This device only requires 8 cm of radial space, is well-suited for our hadronic particle identification requirements, and may be possible to obtain from SLAC. An inner part of the calorimeter for DVCS photons could be placed along the solenoid wall to complement a large calorimeter on the the outside of the solenoid.

2. Baryon Endcap

The baryon endcap would be built around the torus. It would consist of drift chambers followed by an electromagnetic calorimeter (optimized for DVCS photons). The inner part of the calorimeter could, however, be optimized for neutron detection.

3. Electron Endcap

The electron endcap could consist of a single region of drift chambers followed by a Cerenkov (threshold or RICH) detector, and an electromagnetic calorimeter. The small-angle part of the calorimeter could be tailored as a low-Q^2 electron tagger, allowing high-resolution charm spectroscopy with quasi-real photons.

IV. ACCELERATOR AND COLLIDER COMPLEX

The accelerator and collider complex will consist of three major components: The CEBAF accelerator will serve as the lepton injector; an IUCF style high current source followed by a Fermilab Project X-like SRF linac will be used for the ions, and the collider itself will consist of two Figure-8 intersecting storage rings with four possible interaction points. The rather conservative estimates summarized in Table II give a design luminosity above 10^{33} cm^{-2} s^{-1} per interaction point for 4 GeV/c protons. The expression for the luminosity in a leption - ion collider is shown in Equation 1,

$$Luminosity = \frac{f_{RF} N_e N_{ion}}{4\pi\beta^*_{ion}} \left(\frac{\beta\gamma}{\epsilon_N}\right)_{ion} \tag{1}$$

where N_e and N_{ion} are the numbers of particles per bunch, f_{RF} is the RF frequency, ϵ_N is the normalized emittance, and $\beta\gamma = p/m$.

The 1.5 GHz RF frequency should not be problematic. At the estimated luminosity, the event rate will be moderate and the random coincidence rate small. The latter can be measured regardless of frequency, or even with a coasting beam. In fact, at constant luminosity, having a

	protons	electrons
RF frequency [GHz]	1.5	1.5
Momentum [GeV/c]	4.00	4.00
γ	4.38	7828
Current [A]	0.8	2.6
Particles per RF bunch	3.33×10^{9}	1.08×10^{10}
Normalized emittance [m rad]	2.0×10^{-7}	1.0×10^{-5}
Geometric emittance [m rad]	4.69×10^{-8}	1.28×10^{-9}
β^* [m]	0.005	0.184
σ^* [m]	1.53×10^{-5}	1.53×10^{-5}
Beam-beam interaction, ξ_i	6.3×10^{-3}	7.5×10^{-2}

TABLE II: Contributions to a luminosity of 2×10^{33} cm^{-2} s^{-1} in 4 on 4 GeV/c kinematics.

three times higher charge per bunch does not make it easier to suppress randoms, which now often originate from multiple interactions within the same bunch rather than the two neighboring ones. As in the CLAS detector, the determination of the event start time can be determined by tracking the scattered electron and would not rely on the RF signal. Should it at some point be deemed necessary, one inject only one out of three beam buckets.

A. Injectors

The lepton injector will use the CEBAF accelerator, and the accumulation scheme can be adapted from the one developed for ELIC. However, since there is no longer a need for strong focusing of the electrons, much larger emittances are acceptable, reducing sensitivity to synchrotron radiation and space charge effects. This not only makes it easier to operate at higher energies (above 6 GeV), but could potentially allow much higher currents than we assumed in our luminosity estimate, by increasing the number of electrons per bunch. Still, considering the limitations of the polarized source and accumulation scheme, it is not clear at this time how much higher one could go.

The ion injector, illustrated in Figure 6, is based on a polarized ion source and stacking/cooling scheme developed at the Indiana University Cyclotron Facility (IUCF), a 2 GeV SRF linac, and a booster ring. Polarized ions from the source will either go through the entire linac into the fixed target area, or only through the first 300 MeV section, after which they can be redirected into a compact (3 meter radius) accumulator ring. When the entire aperture is filled, the ions will be cooled by a 200 keV DC electron beam with a characteristic damping time of 0.01 s, upon

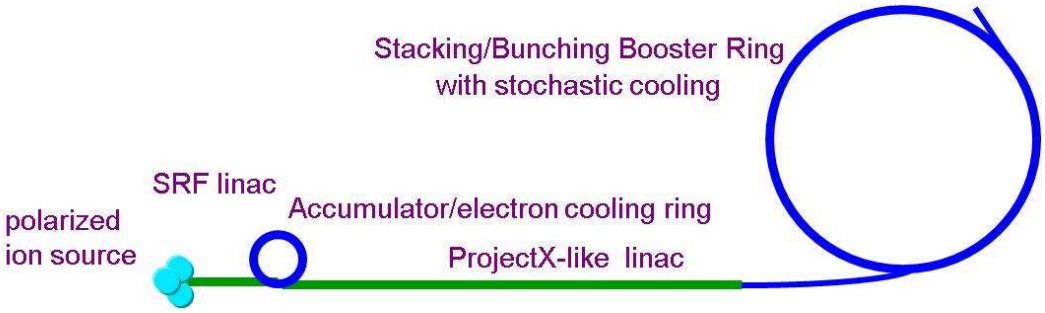

FIG. 6: *Project X based ion injector.*

which the next ion beam pulse will be injected and subsequently cooled. Accumulation of a 80 mA ion beam would take about a second [22], after which the ions will continue into the second stage of the linac on their way to the booster ring. The use of a linac for initial acceleration allows one to deliver much smaller emittance than could be achieved in a ring. Components for the SRF linac are already being developed at Jefferson Lab for Project X at Fermilab. The Project X linac is designed for 8 GeV, but a 2 GeV section at Jefferson Lab could serve as a prototype for the low-β part. The linac would operate in CW mode, which would also be favorable for the neutrino factory that is being planned at Fermilab.

To increase the current to the Ampere range, ions from the linac will be injected into an accumulator/booster ring. The suggested scheme for this process is to use polarized negatively charged ions (H^-), which are stripped of their electrons during multi-turn injection, allowing "phase space painting". This would result in a 2 GeV coasting beam with space charge limited emittance. To reduce the emittance, stochastic cooling would be employed, for which the equilibrium emittance improves with as the beam energy increases. After cooling, the RF system would be used to give the beam the appropriate time structure, upon which the magnets would be ramped and the beam accelerated to the desired energy. This could be followed by a second stage of bunched beam stochastic cooling - a technique being developed for the RHIC upgrade - as the final emittance suppression. It should also be mentioned that the booster ring could take advantage of an alternative to the multi-turn injection stacking scheme described above to further increase bunch intensities. The so-called bunch coalescing scheme (similar to the one used at Fermilab's Main Injector) uses two RF systems to merge 10 bunches into one. This scheme can also work with positive ions, should the intensity of such sources make them an attractive alternative.

B. Collider Rings

In order to avoid depolarizing resonances, the collider ring complex would consist of two vertically stacked identical Figure-8 rings of about 900 m in circumference, including two 150 meter long crossing straight sections accommodating two pairs of interaction regions (IR). Significant

design efforts has been made to develop such lattices for ELIC [5]. One can use a scaled down version of that lattice for the new collider.

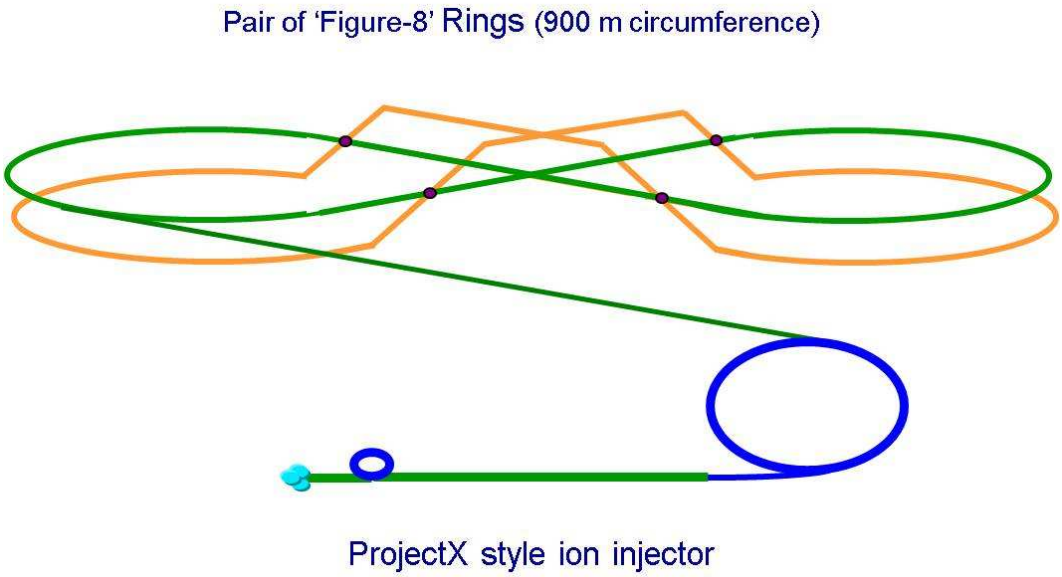

FIG. 7: *Collider rings and ion injector.*

The ring optics is built up from compact FODO structures of 60° or 120° betatron phase advance per cell for ions and electrons respectively. A high (over 60%) dipole packing factor guarantees small momentum compaction ($\alpha \sim 10^{-4}$) to alleviate bunch lengthening and limit RF needs (to about 1 GV) [23]. Each half arc of the Figure-8 forms a minimum dispersion achromat in which dispersion is suppressed by the "missing dipole" technique (*i.e.*, purely geometrically with no change to Twiss function periodicity), which has great impact on the chromatic stability of the lattice [24]. The polarized electron beam will be supplied by the CEBAF Recirculating Linear Accelerator, where electrons from a ($> 80\%$) polarized photo-injector are accelerated to energies of up to 8.8 GeV and then injected into the Figure-8 collider ring with a vertical polarization. To achieve a longitudinal polarization at the IRs, required by some physics experiments, the vertical crossing dipoles can be utilized for a portion of the required spin rotation. A scheme of "energy transparent" spin rotation has been proposed that utilizes horizontal arc dipoles and superconducting solenoid spin rotators to ensure longitudinal polarization at the IRs [25].

C. Interaction Regions

Despite a similarity in the optics design for Figure-8 collider rings, the four interaction regions (IR) will be significantly different than in the ELIC design, where the strong focusing was required for both electron and ion beams. The very aggresive β^* of 5 mm, combined with a very

small crossing angle of 22 mrad was only achievable with interleaved doublets. A more effective triplet based final focus could not be applied due to transverse magnet interferences. The IR was thus limited by very strong superconducting quads for ions and large apperture normal conducting quads for the electrons, occupying approximetely the same location. This was accommodated by specially designed Lambertson quads (with a pass through field free region for the other beam).

Using asymmetric focusing (still extermely strong for the ions but rather weak for electrons), this undesirable and technologically complex arrangement can be replaced by two independent triplet-based final focus systems: an inner one for the ions and an outer for the electrons. Due to lower ion momenta, the 250 T/m superconducting quads planned for ELIC will be replaced by regular 10 T/m quads, where the aperture size can be made quite large (several centimeters). The latter is necessary since the maximum transverse size of the beam, given by $\sigma^{max} = \sqrt{\beta^{max}\epsilon_N/\beta\gamma}$, where ϵ_N is the normalized emittance and $\beta\gamma = p/m$, increases at low momentum. The focal length f, determining the size of the interaction region, is in the thin lens limit $f = \sqrt{\beta^* \beta^{max}}$. As shown in Figure 8, even with the improved triplet optics β^{max} reaches 35 km for an 8 m long IR. Reductions in β^* beyond 5 mm do not seem feasible because of the very large beam envelopes and strong chromatic effects.

The conflicting requirements on the strength and apertures of the quadrupole magnets incidentally also restricts operations of ELIC to very high energies. In ELIC, the minimum energy cannot be lowered by further reducing the size of the interaction regions (f). The only way to limit σ^{max} to fit the aperture of the superconducting quads is to dramatically increase the β^* of the ions, causing a drop in luminosity as shown by Equation 1.

The lower ion momenta also greatly simplify the crab crossing. Since the voltage of the crab cavities increases proportionally to the particle momentum and rotation angle, achieving even a 22 mrad angle between the beams in ELIC assumes that 24 MV cavities can be developed for the ions - a considerable challenge considering that existing cavities, such as the 1.8 MV ones at KEK, are an order of magnitude weaker. Even so, the small design angle and separation distance requires a hole in the yoke of the superconducting quads for the beam to pass through. In our proposed design, the crossing angle can be increased so that the electrons can pass on the outside of the ion quads, and at a voltage well within the capabilities of standard cavities.

Another advantage of the proposed design is that ion IR optics will have a ten times smaller (better) longitudinal acceptance ($\delta p/p \sim 10^{-4}$) than the electrons at ELIC, but with the same low β^*, some level of chromatic corrections will still be required. As demonstrated in Ref. [26] for ELIC, the chromatic effects of the FF quads can be effectively corrected by two families of sextupoles placed symmetrically around the IR in a dispersive region. A confined dispersion wave is launched by a four-bend-chicane used to create the vertical crossing. Undesired spherical aberrations introduced by the sextupoles are mitigated by design, via a dedicated optics, which features an inverse identity transformation between sextupoles in each pair. In addition, the optics guarantees sextupole orthogonality in both planes, which in turn minimizes the required sextupole

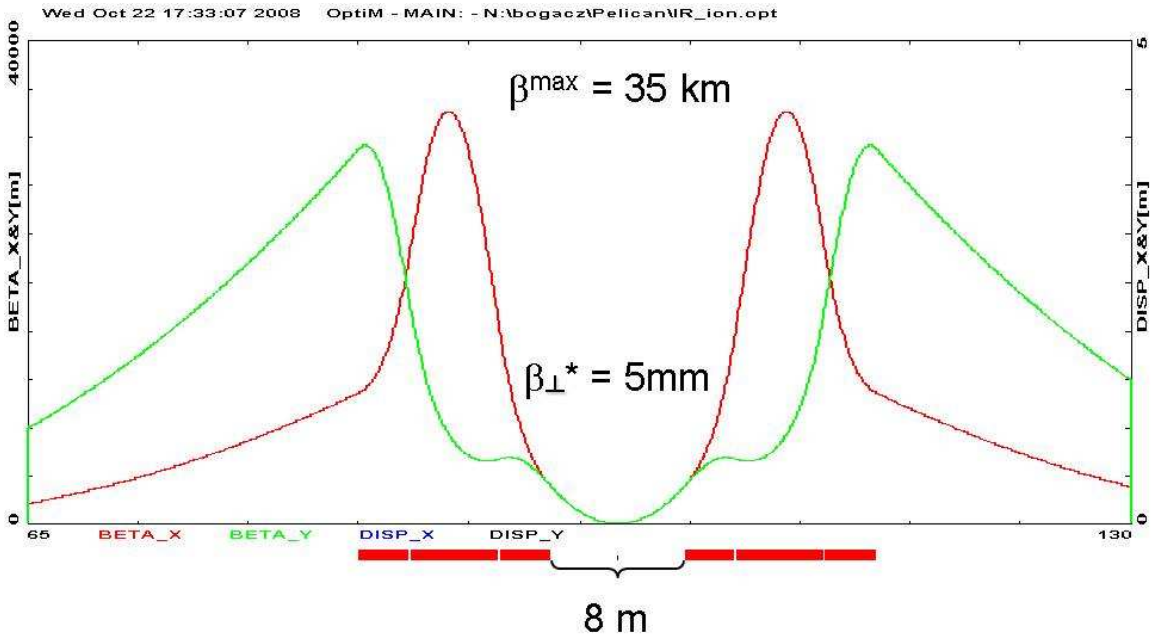

(a) *IR ion optics*

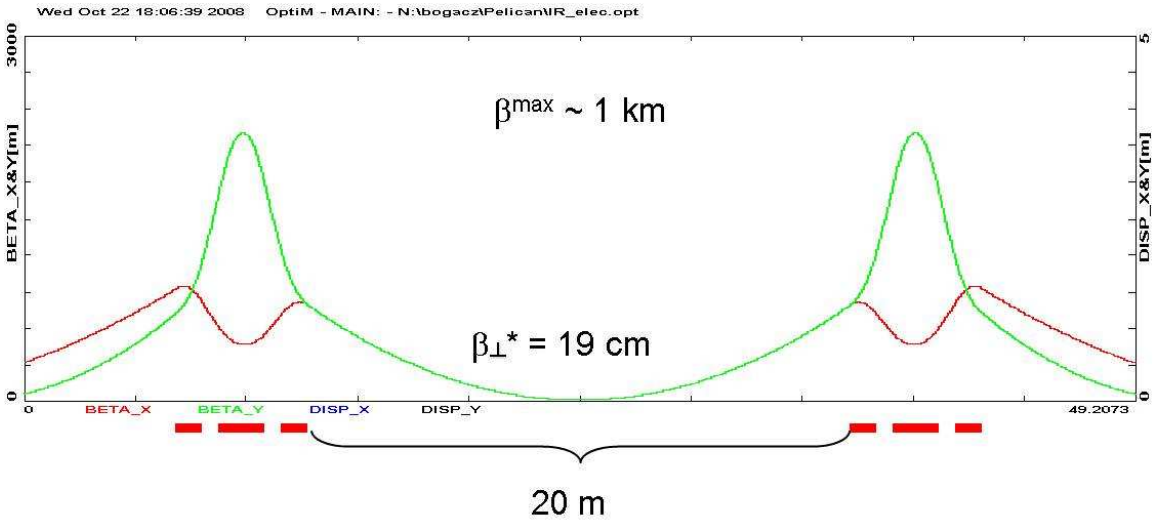

(b) *IR electron optics*

FIG. 8: *Asymmetric focusing.*

strength and eventually leads to larger dynamic aperture of the collider.

V. STAGED CONSTRUCTION AND UPGRADE PLAN

While one could build the proposed collider in one step, a staged approach may be preferable. Two options are presented. The first one offers lower starting costs, a simpler booster ring, and more opportunities for fixed target applications. The second is a slightly cheaper version of the complete collider, with some upgrade potential.

A. Option 1: Linac First

In this option the full potential of the collider will not be available until the advent of the polarized ion injector, but the steps outlined below would each open up a qualitatively different set of physics opportunities, allowing a steady stream of results to emerge even if funding is provided over a long period of time. The cost estimates are very preliminary, and primarily intended for a relative comparison.

- 2 GeV/c ion linac and fixed-target experimental area.
- 8.8 on 2 GeV/c collider (40 GeV on fixed target) with unpolarized ions and low luminosity.
- Polarized ion source and injector providing at least 9 GeV/c ions with luminosities of $10^{33} - 10^{34}$ $\mathrm{cm}^{-2}\mathrm{s}^{-1}$.
- Detector upgrades

Note the stages could also easily be combined. For instance, one could merge the two in the middle, building the collider from the outset with the polarized, high-luminosity ion injector. The details of each stage are summarized in their separate sections.

1. Proton Linac and Fixed Target Area

- Ion linac providing 80 mA of 2 GeV/c protons. (*estimated cost: $ 50 M)*
- Unpolarized high-current ion source. (*estimated cost: $ 5 M)*
- Beamline and fixed target areas for both basic and applied research.

The goals of the first stage would be to build the 2 GeV section of the ion linac as soon as it becomes available, serving as a technology demonstrator (see section VI) and prototype for Project X. An unpolarized ion source would make it possible to run high currents (*i.e.*, high power).

A sequential experimental area would also be built. The upstream part would have gas targets providing a high luminosity, but having little impact on the beam. Such targets exist and could, together with entire experimental setups, be transferred at minimal cost from nuclear physics facilities that are ending their operations. Such setups could, for instance, include ANKE

or WASA from COSY. This would not only allow high quality low-energy nuclear physics to be conducted from the beginning of the upgrade, but also attract a new hadronic user community, which later could become part of the collider program. With many smaller facilities closing, the fixed target area at Jefferson Lab would fill an important void.

For the downstream part there would be a wide range of options, again attracting a new user community. The main focus would be on applied science and industrial applications. The construction can be staged, and expand naturally as this user community grows. Some options are discussed in section VI below.

2. Collider with Unpolarized Ions

- Intersecting storage rings. (*estimated cost: $ 20 M)*
- Accumulator ring for lepton injector. (*estimated cost: $ 10 M)*
- Simple detector for storage ring. (*estimated cost: $)*

If built as a separate stage, this simple version of the collider would inject the linac beam straight into the storage ring using a high-current unpolarized ion source, partly compensating for the lack of the accumulator/booster ring. With unpolarized electrons it might be possible to raise the electron current as well. The center-of-mass energy would be comparable to the 4 on 4 GeV/c case discussed earlier, but as shown in Figures 9-11, the kinematics would be less favorable. The exception would be that it would be easier to detect baryons at low $-t$ without bending them out, making it possible to use a much simpler detector setup. If one would need to build the collider in two steps, the first detector could be made relatively inexpensive.

While the lower luminosity would restrict experiments to low Q^2, some interesting results could still be obtained. Examples could include spectroscopy with quasireal photons and inclusive measurements.

3. High-Luminosity Collider with Polarized Ions

- Polarized ion source. (*estimated cost: $ 10 M)*
- Small ring for electron cooling. (*estimated cost: $ 2 M)*
- Booster ring. (*estimated cost: $ 40 M)*
- Detector for the storage ring. (*estimated cost: $)*

This would be the definitive version of the collider, offering a wide range of physics options. At least one fully equipped detector would have to be built.

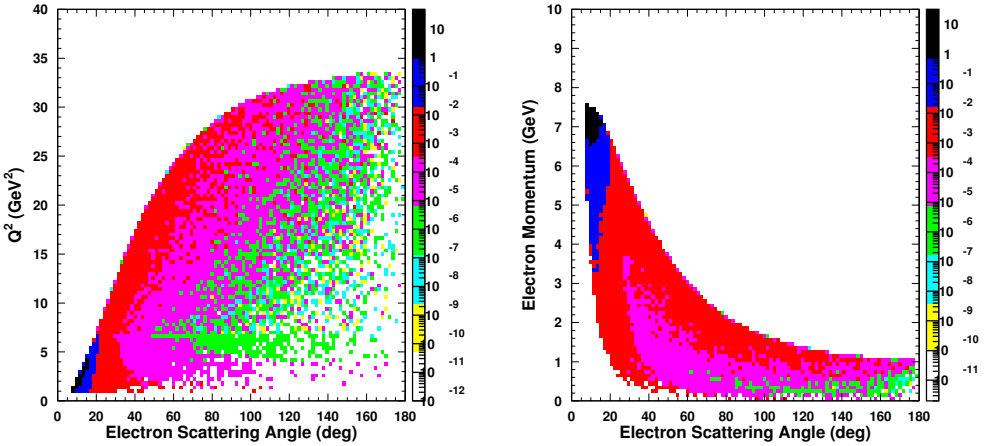

(a) Q^2 *vs. scattering angle* (b) *p vs. scattering angle*

FIG. 9: *8.8 on 2 GeV/c electron kinematics.*

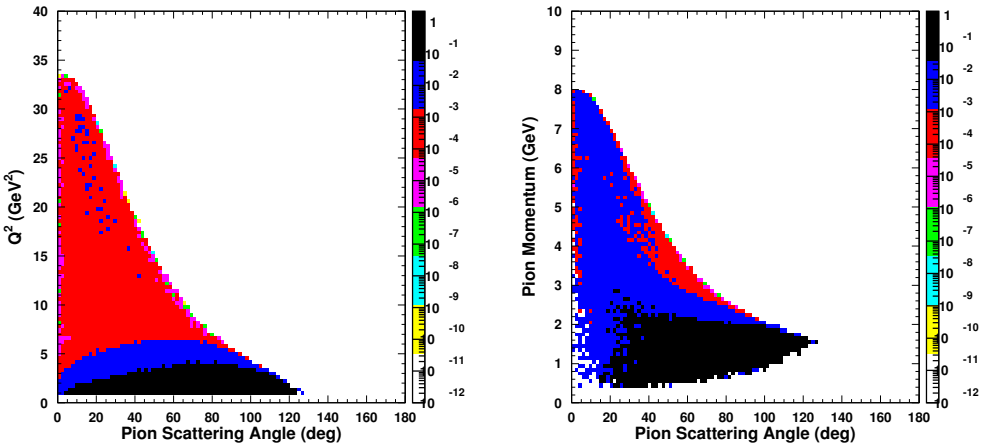

(a) Q^2 *vs. scattering angle* (b) *p vs. scattering angle*

FIG. 10: *8.8 on 2 GeV/c pion kinematics.*

4. Detector Upgrades

• Detector upgrades, or new detector(s) for remaining interaction regions.

Since there would be four interaction points on the ring new detectors can be added without scrapping the earlier ones when new needs arise, although in some cases upgrades can be preferable.

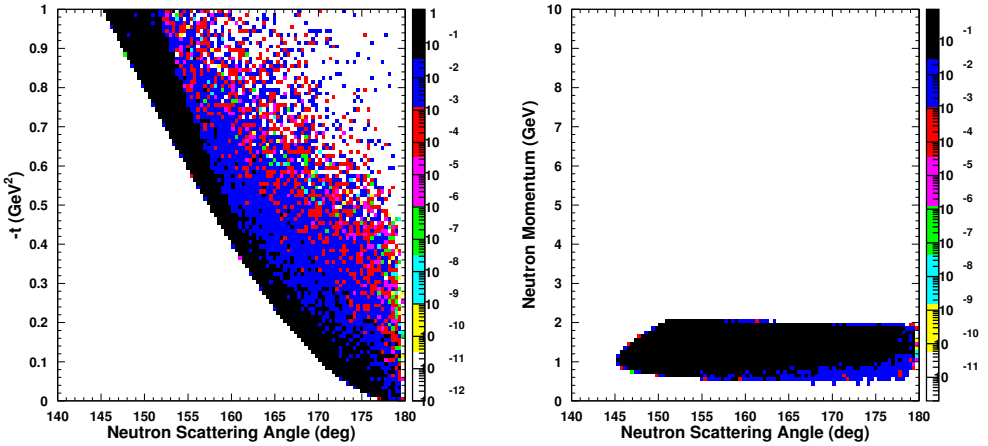

(a) $-t$ *vs. scattering angle* (b) p *vs. scattering angle*

FIG. 11: *8.8 on 2 GeV/c neutron kinematics.*

The flexibility to add detectors over time would allow a certain flexibility in the funding.

B. Option 2: Collider First

This option would require tbe collider complex to be built from the beginning. It would, however, initially only include the first 300 MeV section of the linac. The beam would be injected into the accumulator ring, where it would undergo electron cooling, and then be transferred directly to the booster ring. Due to the low energy, stochastic cooling could only be applied after bunching and acceleration, but due to the bunched beam its efficiency would be limited. While this scheme would not provide as good an emittance as the original one, it would reduce the cost of the injector by shortening the linac. Since the linac energy would be too low for most applications, initially a simple ion beam dump would be built.

In a second stage, the linac energy could be increased to 2 GeV. The injection into the booster ring would be modified to take advantage of the upgraded linac, and stochastic cooling would be added to the booster ring itself. Finally, the beam dump could be replaced by a fixed target area.

Should it be decided not to upgrade the linac, an RF system with a capability to do bunching and acceleration could be added to a larger version of the accumulator ring. During injection into the booster at an energy suitable for stochastic cooling, one could recreate a coasting beam, which again would be bunched and possibly accelerated.

VI. APPLICATIONS

A. Transmutation of Nuclear Waste

The technology of reliable high-current, CW linacs is by itself an important application. With energy independence and global warming being among the most important challenges of the next couple of decades, nuclear energy is likely to be a part of the solution. Still, at this time there is no final plan for dealing with the spent fuel. An important method for reducing the needs for long term storage is transmutation of nuclear waste. Exposing used fuel, no longer able to sustain a chain reaction in a standard water moderated reactor, to an intense flux of neutrons, causes multiple captures and fission. The result is a mix of isotopes with much shorter lifetimes and with a sufficient content of heavy plutonium isotopes to make it unsuitable for use in nuclear weapons. Currently, transmutation research mainly focuses on reactors using fast rather than thermal neutrons. While simpler and cheaper than accelerator driven systems (ADS), such reactors lack some of the passive safeguards of water moderated ones, where boiling water reduces the neutron flux (negative void coefficient), and a rise in temperature also reduces the thermal neutron flux by an increased capture rate in U-238 due to Doppler broadening. Even with advanced control systems, a fast breeder or transmutation reactor may thus be perceived as unsafe compared with regular power reactors. A subcritical system, on the other hand, operating by multiplication of neutrons from a spallation source, could be much easier to accept. It would thus seem prudent for DOE to develop the skills in building and operating high-power accelerators to the level where they reach the reliability required for industrial applications.

B. Long-Pulsed Spallation Neutron Source

An intriguing application of a high-power proton linac is doing neutron physics using a spallation source. A 1.4 MW short-pulsed one, designed for time-of-flight measurements, exists in the US at Oak Ridge (SNS). However, many techniques benefit more from a higher flux. A long-pulse source would thus form a very important complement. This was recognized in the European Spallation Source (ESS) project [10], which presents a comprehensive and compelling case for the science and applications. The problems is only that as a standalone laboratory, on top of costs for land and infrastructure, it requires a dedicated 5 MW proton linac, which in turn cannot be motivated unless very extensive experimental areas are built up from the start. This results in a price tag that may prevent it from ever materializing.

At Jefferson Lab the situation would be very different, since the linac and much of the infrastructure (for instance helium for the superconducting cavities), will already be in place. The only major additional investment would be the spallation target. As a consequence experiments can be built up over time, depending on the needs and funding of the user community and industrial

partners. The proposed linac could deliver 0.5 MW from a polarized ion source. With unpolarized protons, the power could increase by an order of magnitude. A Jefferson Lab spallation source could thus provide a basic capability in many ways comparable to the ESS, but at a small fraction of the cost.

C. Industrial Applications

Regardless of the scale of the downstream proton target area, it will be possible to use the facility for certain industrial applications. Even a simple source could, for instance, be used for studies of Single Event Upsets in microelectronics [27]. As components are miniaturized, the ionization created by a recoiling silicon nucleus, or reaction products following an interaction with a neutron, can affect its functionality (a processor may, for instance, give the wrong answer), long before permanent damage is done to the material. Exposure to such neutron fluxes is largest in high-flying commercial and military aircraft, and the industry has shown a growing demand for testing of its products [28, 29]. Military applications may also require testing of components for exposure to man made sources. Such a facility at Jefferson Lab could thus provide a source of revenue.

Another important energy application could be in developing materials for future fusion energy facilities, where the neutron fluxes will be orders of magnitude higher than in conventional fission reactors, and thus present a new set of construction challenges.

It would also be possible to use such a facility for accelerator-driven production of tritium (ATP).

An additional application of this facility could be a contribution to the Stockpile stewardship program. Currently, the task of stockpile maintenance relies on the use of simulations, and the construction of specialized science facilities has often be criticized as inefficient as they are expensive to build, and are not expected to make significant contributions to the maintenance of US nuclear capabilities. At Jefferson Lab, much of the needed infrastructure would be in place, and supporting experiments could be constructed as the need arises.

VII. ADDING COSY TO CEBAF

One possibility of reducing the construction costs of the proposed collider would be to use component from COSY. However, while the idea may at first seem appealing, a closer inspection reveals many problems.

To use COSY as part of the collider, one would have to give up the polarization advantage of a Figure-8 design. Furthermore, the RF system would have to be replaced as it operates at the wrong frequency. The time structure is appropriate for fixed targets but not colliders, where the very long bunches would produce a large hourglass effect, dramatically reducing the luminosity. To

use COSY as a collider, the optics would need to be redone from scratch, and the injector cyclotron would have to be replaced. From a cost saving perspective, this basically leaves the beam pipes and dipoles. However, the dipoles would only be be suitable for energies below 3.7 GeV, creating a significant limitation with no prospects for future upgrades.

A recent study of a COSY-based collider [11], presented after our initial estimates, also shows that the luminosity would be at least an order of magnitude lower than our proposed design. The assumptions made in that study were very optimistic and the nominal number that was presented matched our conservative estimate. The discrepancy can be understood in terms of the effect of two parameters, related to the interaction point optics and a new CEBAF accumulator ring required to raise the number of electrons per bunch from millions to tens of billions. Neither one of these parameters has anything to do with COSY and can be made identical in both concepts. The result, however, is that either one has to increase our luminosity to 2×10^{34}, or reduce that of the COSY-based design to 2×10^{32}. Unfortunately, the latter seems more realistic. The two parameters and their effect are discussed in the two paragraphs below.

The first assumption, giving a factor of two, was that the focusing at the interaction point can be made twice as strong by reducing β^* for the ions from the already controversial 5 mm used in ELIC to 2.5 mm (colliders typically have β^* in the 100 - 500 mm range). As discussed in Section IV C, this would put unrealistic requirements on the aperture size of the quads, shrink the already small interaction region (measured quad-to-quad, not by the length of the straight-section), and introduce strong chromatic effects.

The second assumption, giving a factor of five, was that the number of electrons per bunch is limited only by synchrotron radiation even at low energies, where the effect is small. This makes the number of electrons very large. While we assume 10.8 billion at 4 GeV, the COSY-based design assumes 45 billion at 5 GeV (it would be more at 4 GeV). It is not explained why one can neglect, for instance, space charge effects, and no explicit scheme for accumulating such bunch charges of polarized CEBAF beam has been suggested. Until an explanation is given of how this can be achieved, we are reluctant to use this very optimistic assumption in our estimates.

An alternative to using COSY as a collider would be in the ion injector. There it could, without costly modifications, serve as an accumulator ring. However, in our proposed design this ring can be made much smaller (with a circumference of $\sim$ 10 m vs. 182 m for COSY), and it would be cheaper to build it from scratch. If one would invest in a new RF system, COSY could be used as a booster ring, but this would again limit the maximum energy to 3.7 GeV. Going beyond that would require a second booster ring, making the COSY part redundant. The only way to fit COSY into our proposal would be in option 2 of our staging plan, where it would replace the second part of the linac. Due to the required upgrades, however, this would at best lead to a marginal overall cost reduction (in particular since the more expensive booster ring would have to be made at least to the same size). Such a solution would also provide inferior performance and no opportunities for fixed-target experiments or applications.

The greatest value of COSY may, however, not be its dipole magnets, but the experiments. These could be used transferred to Jefferson Lab for use in the fixed target area. Beam pipes, diagnostics, ion sources, and parts of the cooling systems could probably be recycled as well.

[1] Y. Derbenev *et al.*, Advanced Concepts for Electron-Ion Collider, Proc. EPAC 2002.

[2] L. Merminga *et al.*, ELIC: An Electron Light-Ion Collider Based at CEBAF, Proc. EPAC 2002.

[3] Y. Derbenev *et al.*, Electron-Ion Collider at CEBAF: New Insights and Conceptual Progress, Proc. EPAC 2004.

[4] Y. Derbenev *et al.*, Concepts for ELIC - A High Luminosity CEBAF based Electron-Light Ion Collider, Proc. RUPAC 2006.

[5] A. Bogacz *et al.*, Design Studies of High-Luminosity Ring-Ring Electron-Ion Collider at CEBAF, Proc. PAC 2007.

[6] D. Prasuhn *et al.*, *Status of the Cooler Synchrotron COSY-Juelich*, Proc. PAC 2003.

[7] Project X Fermilab Acclerator Advisory Committee Review Report, 2007, *http://projectx.fnal.gov/AACReview/index.html*.

[8] Draft ILC Reference Design Report, April 2007.

[9] SNS parameters list, 2005, *http://neutrons.ornl.gov/pubs/*.

[10] I.S.K. Gardner *et al.*, The ESS Project Volume III Update, Technical Report Status (2003), *http://neutron.neutron-eu.net/n_documentation/n_reports/n_ess_reports_and_more/106*.

[11] Y. Derbenev, G. Krafft, and Y. Zhang, *A Polarized Electron-Ion Collider based on CEBAF and COSY*, (2008).

[12] D. Cassel, *Lattice QCD and CLEO-c tackle the CP challenge*, CERN Courier, 18 July 2005.

[13] I.S. Barker, A. Donnachie, and J.K. Storrow, Nucl. Phys. **B95**, 347 (1975).

[14] A. Bogacz *et al.*, Interaction Region Design for the Electron-Light Ion Collider ELIC, Proc. PAC 2005.

[15] COMPASS parameters list, 2005, *http://wwwcompass.cern.ch*.

[16] B.A. Mecking *et al.*, Nucl. Instrum. and Methods **A503** 513-553 (2003).

[17] B.Q. Ma, Phys. Lett. **B274** 111 (1992).

[18] C. Lippmann, the ALICE TPC collaboration, arXiv:0809.5133 (2008); P. Glaessel, for the ALICE TPC Collaboration, Nucl. Instrum. and Methods **A572** 64-66 (2007).

[19] J. Schwiening, Nucl. Instrum. and Methods **A502** 67-75 (2003).

[20] Y. Derbenev *et al.*, Use of an Electron Beam to Stochastic Cooling, Proc. COOL 2007.

[21] A. Deshpande, R. Milner, R. Venugopalan, and W. Vogelsang, Annu. Rev. Nucl. Part. Sci. **55** 165-228 (2005).

[22] X. Pei, Ph.D. thesis, Indiana University, (1991).

[23] A. Bogacz, JLAB-TN-06-051.

[24] A. Bogacz, JLAB-TN-06-052.

[25] A. Bogacz *et al.*, Electron Spin Rotation and Spin Matching Schemes for ELIC, SPIN08.

[26] A. Bogacz *et al.*, Advances on ELIC Design Studies, EPAC08.

[27] P. J. Griffin *et al.*, *The role of thermal and fission neutrons in reactor neutron-induced upsets in commercial SRAMSs*, IEEE NS Vol. 44, No. 6, Dec. 1997.

[28] C. I. Underwood, *The Single-Event-Effect Behaviour of Commercial-Off-The-Shelf Memory Devices - A Decade in the Low-Earth orbit*, IEEE Transactions on Nuclear Science Vol. 45, No. 3, June 1998.

[29] G. R. Srinivasan, *Parameter-free predictive modeling of single event upsets due to protons, neutrons*

and pions in terrestial cosmic rays, IEEE Transactions on Nuclear Science Vol. 41, No. 6, Dec. 1994.